Proc. Natl. Acad. Sci. USA
Vol. 82, pp. 7149–7153, October 1985
Neurobiology

The Ca channel in skeletal muscle is a large pore

(ion selectivity/pore size/permeability/organic cations)

E. W. McCLESKEY* AND W. ALMERS†

Department of Physiology and Biophysics, University of Washington SJ-40, Seattle, WA 98195

Communicated by C. L. Prosser, June 27, 1985

ABSTRACT **The permeability of Ca channels to various foreign cations has been investigated in the absence of external Ca^{2+}. All physiological metal cations are clearly permeant, including Mg^{2+}. The large organic cation *n*-butylamine^{+} is sparingly permeant or impermeant, but its larger derivative 1,4-diaminobutane^{2+} is highly permeant. Among the cations of the methylated ammonium series, permeability diminishes in a graded fashion as ion size increases. Tetramethylammonium, the largest cation found to be permeant, has a diameter of about 6 Å; hence, the aqueous pore of the Ca channel at its narrowest point can be no smaller. That the pore is so large strengthens our view that, under physiologic conditions, the high selectivity of Ca channels is due to selective binding of Ca^{2+} rather than to rejection of other cations by, for example, a sieving mechanism.**

Calcium channels in cell membranes are pores that allow the influx of Ca^{2+} in response to membrane depolarization and thereby help produce the increase in intracellular Ca^{2+} that triggers a variety of Ca-dependent physiologic processes, including transmitter release in neurons and contraction in muscle. Under physiologic conditions, Ca channels are extraordinarily selective and exclude the cations Na^+ and K^+ (1–4), even though these are present at comparatively much higher concentrations. When extracellular Ca^{2+} is absent, however, Ca channels become freely permeable to many monovalent cations. This applies to Ca channels generally, as the effect is observed in Ca channels from different tissues, such as neurons (5), muscles (6–8), lymphocytes (4), and oocytes (9), as well as from different phylae, such as vertebrates (4, 6, 7), arthropods (10), and molluscs (5). The well-known high permeability of Ca channels to Ba^{2+} similarly depends on the absence of Ca^{2+} (6, 7). Apparently the selectivity of the Ca channel shows itself only when Ca^{2+} occupies a specific site of high affinity (3–6). The selective permeability of Ca channels is evidently based on the selective binding of Ca^{2+}.

The binding of Ca^{2+} almost certainly occurs within the channel, since the block of monovalent cation permeability by Ca^{2+} shows the characteristic voltage dependence expected when a permeant ion blocks by temporarily binding within the aqueous pore (4). In analogy with the mechanism of ion permeation established for the ion channel formed by gramicidin A (11–14), the Ca channel has therefore been viewed as an aqueous pore through which ions move in single file, binding in succession to two Ca-specific sites. In quantitative agreement with experimental data, calculations with this model (6, 7) have shown that such a two-site pore may, in ion mixtures, selectively transport the ion that is bound with the highest affinity. No structural change is required for the Ca channel to first pass and then reject monovalent cations; the binding of Ca^{2+} to a site in the pore is sufficient.

Following the observation on snail neurones (5) that hydrazine may pass through Ca channels, we have investigated the permeability of a variety of organic cations. We report that, in the absence of a high-affinity ion such as Ca^{2+}, the permeability of an ion is determined mainly by its size. From the size-permeability relationship and the size of the largest permeant cation, we deduce the pore size of the Ca channel. A preliminary account of this work has been published (15).

MATERIALS AND METHODS

Segments of single fibers about 3 mm in length were dissected from the semitendinosus muscle of *Rana temporaria* frogs and mounted in a Vaseline gap (16) chamber such that the length in the recording pool (gap width) was 250–650 μm. The fiber ends were immersed in an "intracellular" solution that contained, unless indicated otherwise, 20 mM $NaCH_3SO_3$, 67 mM tetraethylammonium EGTA [$(Et_4N)_2EGTA$], and 10 mM Mops (pH 7.0). Experiments started 30 min after cutting the fiber ends in this solution; this is expected to allow sufficient time for equilibration with the myoplasm by diffusion through the cut ends.

Membrane currents were recorded at 10–13°C under voltage-clamp conditions, corrected for capacitive and leakage currents by a combination of analog and digital techniques (3), and referred to unit fiber surface. Holding potential was −100 mV, and recovery periods of >30 s were allowed between successive depolarizing pulses. Averages are given as means ± SEM.

The "extracellular" solutions applied to the recording pool were designed to prevent current through the ion channels that are responsible for the physiologic resting and action potentials and were based on a standard containing 80 mM $Et_4NCH_3SO_3$, 20 mM $(Et_4N)_2EGTA$, 3 mM $Ca(CH_3SO_3)_2$, 10 mM Et_4N^+/Mops (pH = 7.0), and 1 μM tetrodotoxin. Methanesulfonates of other cations were substituted for $Et_4NCH_3SO_3$ on an isosmolar basis as indicated. $CH_3SO_3^-$ was chosen as the main anion because it is impermeant in Cl channels, as is H_2EGTA^{2-}. Tetrodotoxin and Et_4N^+ were included to block voltage-dependent Na and K channels as well as the inward rectifier K channel responsible for the K permeability of the resting muscle membrane. Our EGTA/Ca mixture buffers free Ca^{2+} to pCa = 7.2, the reference condition in previous work (3). Extracellular solutions were changed by flushing 5–10 ml through the recording pool (0.25-ml capacity) within about 30 s. In some experiments, the Ca-channel blocker nitrendipine (NTP) (a gift from A. Scriabine, Miles Institute) was added from a 1 mM ethanolic stock solution.

NH_4OH, CH_3NH_2, hydrazine, aminoguanidinium bicarbonate *n*-butylamine, 1,4-diaminobutane, and CH_4SO_3 were

The publication costs of this article were defrayed in part by page charge payment. This article must therefore be hereby marked "*advertisement*" in accordance with 18 U.S.C. §1734 solely to indicate this fact.

Abbreviations: Me_4N^+, tetramethylammonium; Et_4N^+, tetraethylammonium; NTP, nitrendipine.

*Present address: Department of Physiology, Yale University School of Medicine, 333 Cedar Street, New Haven, CT 06510.
†To whom reprint requests should be sent.

from Aldrich; $(CH_3)_2NH$, $(CH_3)_3N$, and methylguanidinium sulfate were from Eastman Kodak (Rochester, NY); and tetramethylammonium hydroxide (Me_4NOH) was from Calbiochem. Except for methylguanidinium sulfate, all of these compounds were neutralized with CH_4SO_3 or, in the case of aminoguanidinium bicarbonate, with H_2SO_4. All except for hydrazine (pK_a = 8.23) had pK_a values of >9, assuring >99% protonation at pH 7.0. [Hydrazinium$^+$] was taken as being 0.95 times the total concentration of hydrazine. The osmolarities of the solutions were measured with a vapor pressure osmometer (Wescor, Logan, UT) and were 215–240 mosM or, with 1,4-diaminobutane, were 265 mosM. The sulfate-containing solutions were adjusted with sucrose to 230 mosM.

RESULTS

Even though none of the ion channels that ordinarily participate in resting and action potentials can carry transmembrane current under our experimental conditions, step depolarizations are accompanied by clearly visible inward currents (Fig. 1). These are carried by the ions indicated on the left in Fig. 1, since they vanish when these ions are replaced by Et_4N^+ (not shown). The Na currents in the upper row of traces in Fig. 1 are known to flow through Ca channels that, at low external Ca^{2+}, become permeable to monovalent cations (6). The same may be assumed for the K and Mg currents in Fig. 1. Increasing Ca^{2+} to 1 μM reversibly diminishes Na and K currents (Fig. 1, column 2); for Na currents, block occurs with 1:1 stoichiometry and an ED_{50} of 0.7 μM (3). Throughout, currents are strongly diminished by the specific Ca-channel blocker NTP [ED_{50} = 0.7 μM for Ca current (17)]. A close analogue of this drug, nifedipine, blocks Na and Ca currents through Ca channels with 1:1 stoichiometry and at identical concentrations (6).

Fig. 1 shows that the Ca channel is permeable not only to Ca^{2+} but also to all other physiologically present metal ions. Reversal potential measurements gave a ratio of K and Na permeabilities P_K/P_{Na} = 1.3 ± 0.04 (n = 6) at 30 mM external Na^+ and K^+ concentrations. Mg currents were 0.1 ± 0.05 times as large as Ca currents at the same concentration and membrane potential, consistent with a previous observation (18). Mg current, too, was blocked by Ca^{2+}, though more Ca was required. In terms of the two-site model for ion permeation, Mg^{2+} evidently competes more effectively for the sites than Na^+ and K^+. If 1 mM Ca^{2+} halved the current carried by 100 mM Mg^{2+}, then Ca^{2+} must have a 100-fold higher affinity for the sites than Mg^{2+}. In reality, the difference in affinities must be even larger, since much of the current with 1 mM Ca^{2+} was probably carried by Ca^{2+} and not by Mg^{2+}.

In Fig. 1, inward current in 100 mM Mg^{2+} turns on an order of magnitude more slowly than in Na^+ and K^+. Activation kinetics in 100 mM Ca^{2+} (not shown) and 1,4-diaminobutane (see Fig. 5) are similarly slow. The reasons for this apparent dependence of activation kinetics on the permeant species are not understood.

Fig. 2 shows six sets of current traces recorded from one cell during voltage jumps of different amplitudes. Each set was recorded with a different external cation, as indicated. All ions except Me_4N^+ are clearly seen to carry inward currents during depolarization. Throughout, currents were strongly reduced both by 1 μM Ca^{2+} and by 1 μM NTP (not shown). Progressing from a to f in Fig. 2, inward currents become larger as methyl groups are replaced with hydrogen until NH_4^+ itself gives currents as large as Na^+. If chemically similar ions are compared, permeation in the Ca channel evidently decreases with increasing ion size.

In Fig. 2a, the inward current tails on repolarization suggest that even Me_4N^+ is permeant. Fig. 3 confirms this and shows membrane currents during steps to the indicated potentials, first in a solution with Et_4N^+ as the only cation, then after substituting 80 mM Me_4N^+ for Et_4N^+, and once again in pure Et_4N^+ solution. With Me_4N^+, inward currents are clearly larger than with Et_4N^+. At potentials where currents in Et_4N^+ are absent (−40 mV), or outward (−30 mV), currents in Me_4N^+ remain inward. Clearly, Me_4N^+ is more permeant than Et_4N^+. The inward currents with Et_4N^+ as the only external cation might suggest that even this ion is permeant. However, more experiments are needed to ex-

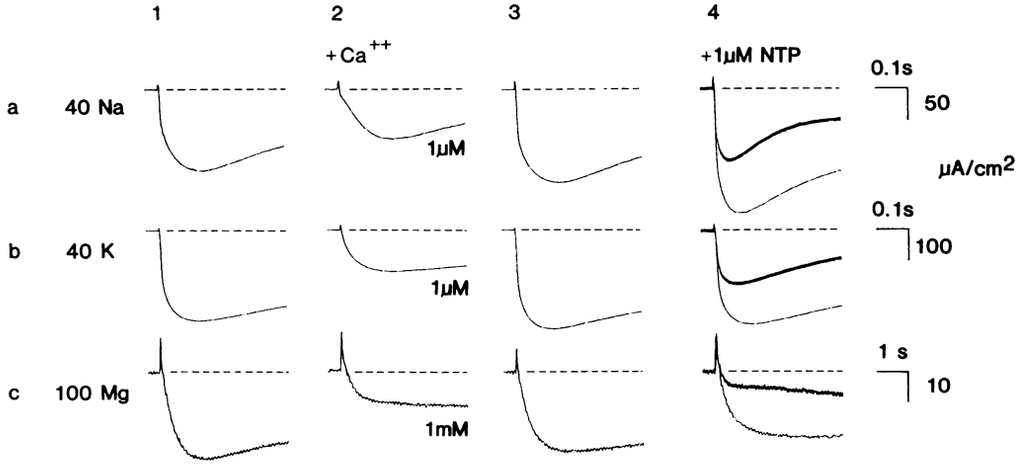

FIG. 1. Currents carried through the Ca channel by Na^+, K^+, or Mg^{2+}. External Ca^{2+} concentration was about 63 nM (a and b) or less (c), except where indicated otherwise. Traces in a, columns 1–3, b, columns 1–3, and c, columns 1–3, were recorded in the sequence shown, each from a different fiber; in a and b, column 2, external Ca^{2+} concentration was increased to 1 μM by adding 14.7 mM $Ca(CH_3SO_3)_2$; in c, column 2, Ca^{2+} concentration was increased to 1 mM as specified below. Column 4, Na, K, and Mg currents recorded just before (light traces) and 30–60 s after application of 1 μM NTP (heavy traces); each panel of traces was from a different fiber. The Na and K currents in a and b were recorded during voltage steps from −100 to −40 mV and with 40 mM external Na^+ or K^+ substituting for Et_4N^+, as indicated; fiber ends were cut in a solution containing 40 mM $NaCH_3SO_3$, 20 mM $(Et_4N)_2EGTA$, 50 mM arginine aspartate, and 10 mM Et_4N^+/Mops (pH = 7.0). Mg currents were recorded during steps from −80 mV to 0 (c, columns 1–3) or to 15 mV (c, column 4); the external solution contained 100 mM $Mg(CH_3SO_3)_2$, 10 mM Et_4N^+/Mops (pH = 7.0), and either 1 mM $(Me_4N)_2EGTA$ or, in c, column 2, 1 mM $Ca(CH_3SO_3)_2$; fiber ends were cut in 80 mM $(Et_4N)_2EGTA$ with 10 mM Et_4N^+/Mops buffer (pH = 7.0). In c, the ordinate calibration applies to columns 1–3 only; for column 4, the calibration bar represents 4 $\mu A/cm^2$.

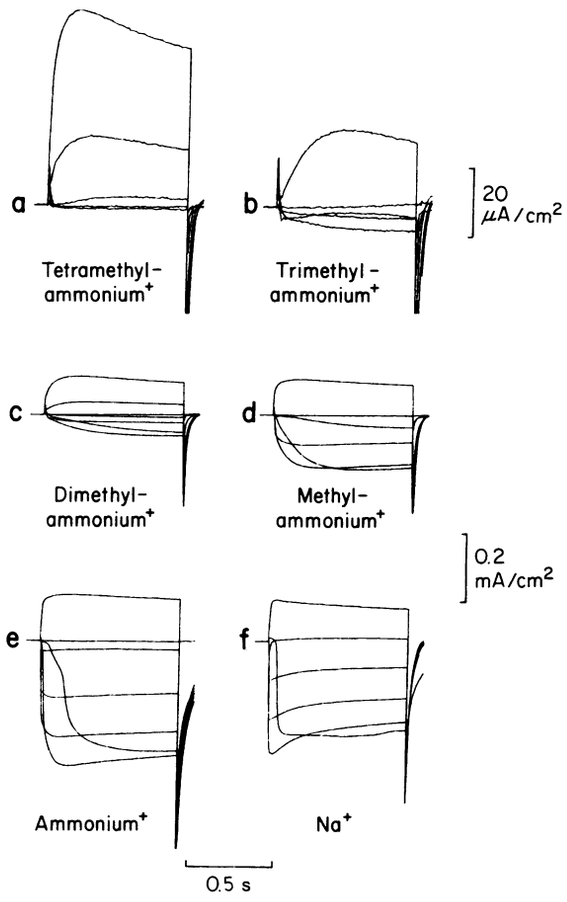

FIG. 2. Membrane currents during jumps to potentials ranging from −80 mV either to 0 mV (*a* and *b*) or to 40 mV (*c–f*) in 20-mV increments, with various external cations substituted for Et_4N^+ as indicated. In *e* and *f*, where currents are large, the irregularities in the current traces at the most negative potentials are probably due to poor potential control in the transverse tubules. In *a* and *b* the tail currents flowing on repolarization to −100 mV were photographically clipped and in reality are larger than the −30 μA/cm² shown. Fiber 6023, gap = 0.56 mm and diameter = 0.08 mm.

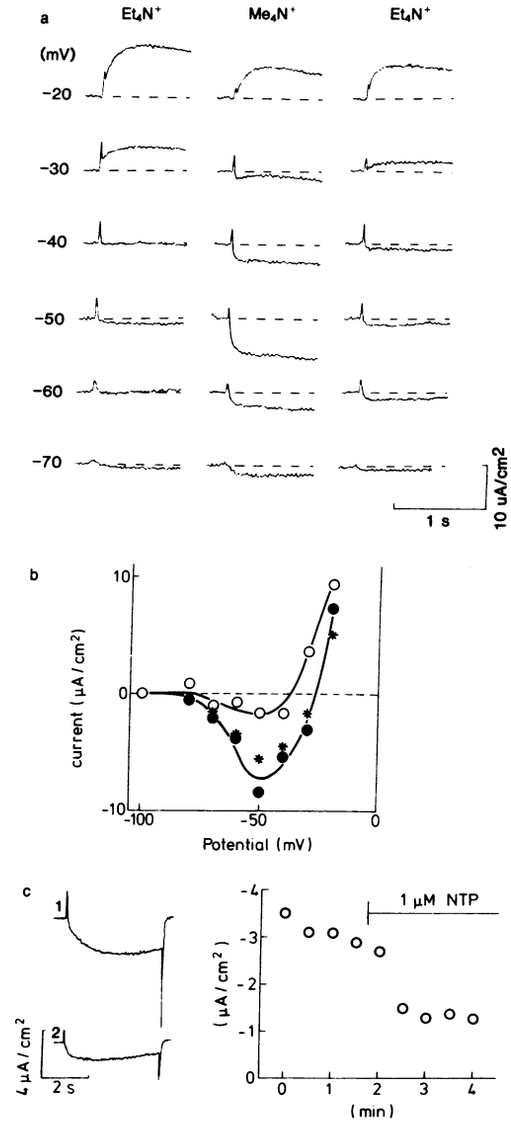

FIG. 3. (*a*) Membrane currents during jumps to the potentials given, with 80 mM Me_4N^+ replacing external Et_4N^+, where indicated. (*b*) Peak current against voltage, with 80 mM Me_4N^+ (●) and 5 mM Na^+ (*) replacing isosmolar amounts of Et_4N^+ (○), as indicated. Solutions were applied in the sequence Et_4N^+, 80 mM Me_4N^+, 5 mM Na^+, Et_4N^+, 80 mM Me_4N^+, 5 mM Na^+; the values plotted are the average from the two runs in each solution. Fiber 6042, gap = 0.51 mm and diameter = 0.1 mm. (*c*) Left: currents with 80 mM Me_4N^+ replacing external Et_4N^+, recorded at −30 mV before (no. 1) and after adding 1 μM NTP (no. 2). The internal solution was as described in the text except that all Na was replaced by Et_4N^+ so that Et_4N^+ was the only cation. Right: peak current plotted against time with 1 μM NTP present as indicated. Fiber 6046, gap = 0.52 mm and diameter = 0.1 mm.

clude that these extremely small inward currents are an erroneous result of leak subtraction.

Fig. 3*b* plots peak current against potential; the values plotted are averages from two bracketing runs each in Et_4N^+, Me_4N^+, and a Et_4N^+ solution containing 5 mM Na^+ (traces not shown). The currents and reversal potentials observed in the 80 mM Me_4N^+ and the 5 mM Na^+ solutions were about the same; hence, Me_4N^+ is 5/80 = 0.06 times as permeant as Na^+ in this experiment. Fig. 3*c* shows that the inward current with Me_4N^+ is partially blocked by 1 μM NTP. Me_4N^+ currents failed to appear clearly in about half of the cells in which we looked for them, probably because these cells contained relatively few Ca channels and consequently produced Me_4N^+ currents that were too small to measure. The content of functional Ca channels is known to be highly variable from fiber to fiber, as judged by the variability of currents through Ca channels (6, 19).

To analyze experiments as in Figs. 2 and 3 we assumed that Et_4N^+ was impermeant and calculated the permeability ratio P_x/P_{Na} by the equation (20)

$$P_x/P_{Na} = \frac{[Na^+]}{[x]} \exp[(V_x - V_{Na})F/RT], \qquad [1]$$

where $[x]$ and $[Na^+]$ denote the external concentrations of the test cation, x, and of Na^+, respectively. F is the Faraday constant, R is the gas constant. T is the absolute temperature, and V_x and V_{Na} are the reversal potentials measured with the two external ions—i.e., the potentials where current changes from being inward to outward. Permeabilities of the ions in Figs. 2 and 3 vary over a 25-fold range, with permeability ratios of 1.50 ± 0.05 (n = 8) for NH_4^+, 1.02 ± 0.03 (n = 5) for $CH_3NH_3^+$, 0.67 ± 0.03 (n = 6) for $(CH_3)_2NH_2^+$, 0.14 ± 0.02 (n = 3) for $(CH_3)_3NH^+$, and 0.055 ± 0.004 (n = 3) for Me_4N^+. Fig. 4*a* plots permeability against ion size. To be consistent with previous work (21), we constructed Corey–Pauling–Koltum models of each ion, determined the volume of the smallest rectangular box that would accommodate it, and calculated the ion size as the length of a cube with that volume. It is seen that permeability diminishes in a graded

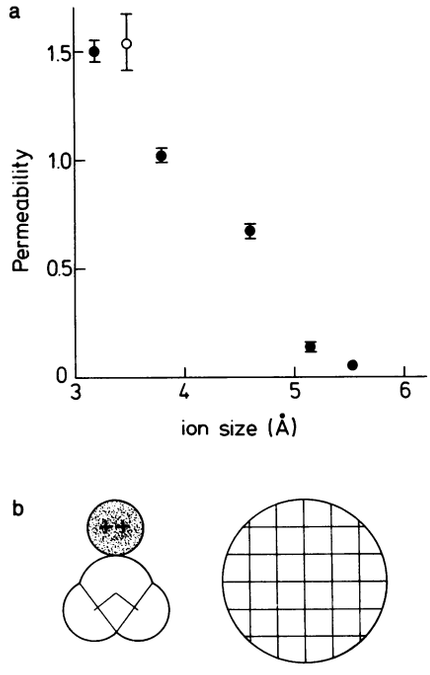

FIG. 4. (*a*) Permeability ratios P_x/P_{Na} of hydrazinium (○) and of ammonium and its four methylated derivatives (●) were calculated from Eq. 1 and are plotted as a function of ion size. Na^+ concentration was 20 mM inside and 20–30 mM outside, except for Me_4N^+, where the comparison measurement of V_{Na} was made with only 5 mM external Na^+ (see Fig. 3*b*). Test cations were applied externally at 80 mM. Measurements of V_x were always bracketed by those of V_{Na}, or vice versa. V_x and V_{Na} were obtained by interpolation from plots of peak current against voltage. Though there may be loss of voltage control in the transverse tubules when currents through Ca channels are large, V_x and V_{Na} should be reliable since they rely on measurements at voltages where these currents are small or zero. SEM is indicated where larger than the symbol. (*b*) Scale drawings of Ca^{2+} and H_2O (left) and a 6-Å pore (right).

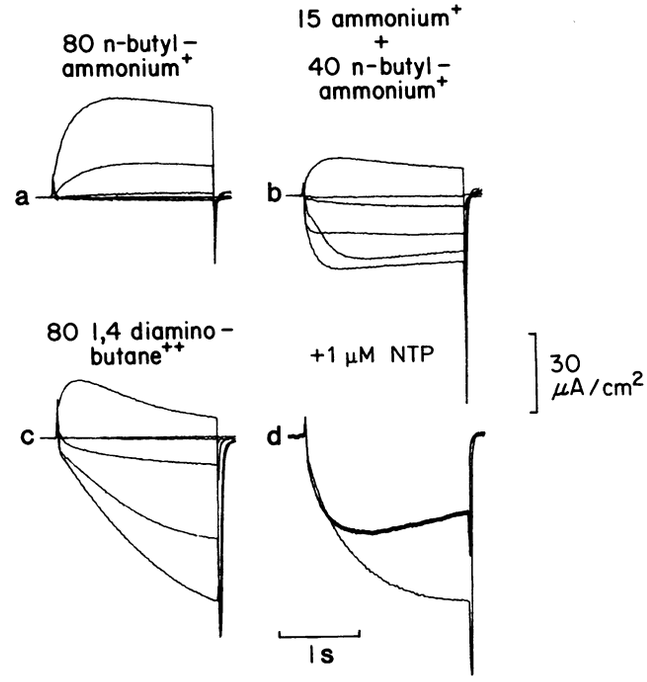

FIG. 5. (*a–c*) Currents at potentials ranging from −80 mV to 20 mV in 20-mV increments recorded in solutions in which Et_4N^+ was replaced by other ions as indicated in mM. (*d*) Currents in a solution as in *c*, recorded at −20 mV before (light trace) and after addition of 1 μM NTP (heavy trace). Fiber 6059, gap = 0.48 mm and diameter = 0.08 mm.

fashion as the ion size increases. Such a relationship between size and permeability is predicted by theories that relate the permeation of spheres through cylindrical tubes to the diameter of the spheres (22). It is consistent with the idea that the Ca channel selects among chemically similar organic cations by a sieving mechanism.

Permeabilities calculated from reversal potentials in some cases disagreed with permeabilities inferred from the amplitudes of inward currents. For instance, methylammonium and Na^+ are equally permeant as judged by reversal potential measurements, yet inward currents were on average twice as large for Na^+. Such disagreements are expected if the pore contains binding sites with different affinities for different ions (6, 7).

In addition to methylated ammonium compounds, the following other cations were investigated: hydrazinium, guanidinium, methylguanidinium, and aminoguanidinium. All were clearly permeant. Hydrazinium was 1.3 ± 0.1 (n = 3) times more permeant than methylamine, and aminoguanidinium was 1.7 ± 0.2 (n = 6) times more permeant than methylguanidinium. It seems that amino groups, which form hydrogen bonds, confer greater permeability than methyl groups, which do not, on otherwise identical ions. A similar result on Na channels has been attributed to oxygen atoms lining the aqueous pore (20).

Fig. 5*a* shows membrane currents in *n*-butylammonium. This ion is highly flexible and would, if coiled together, be approximately as large as Me_4N^+. No inward currents are apparent at the gain employed, indicating that *n*-butylammonium is either impermeant or that its permeability is small, as with Me_4N^+. Absence of large inward current in *n*-butylammonium could be explained if this ion bound tightly to a site within the channel, perhaps by virtue of its lipophilic side chain. If so, *n*-butylammonium should block the channel, but this was not observed. In Fig. 5*b*, large ammonium currents are seen despite the presence of 40 mM *n*-butylammonium. In another fiber, comparison of ammonium current with and without 40 mM *n*-butylammonium showed essentially no difference in inward current. Evidently, *n*-butylammonium does not cause significant block of the Ca channel.

Surprisingly, the larger ion 1,4-diaminobutane gives a clear inward current (Fig. 5*c*) that is blocked by NTP (Fig. 5*d*). At pH 7.0, diaminobutane is divalent with charged amino groups on both ends of the butane backbone. Evidently, the addition of a second cationic group has strikingly increased the permeability. Perhaps electrostatic repulsion between the two charged groups keeps this molecule extended so it can pass lengthwise through the channel. In addition, a negative surface potential near the external channel mouth would tend to increase the local concentration of 1,4-diaminobutane^{2+} more than that of *n*-butylammonium$^+$. Both factors in combination would allow the divalent derivative to pass larger inward currents than its monovalent parent compound. The high permeability of 1,4-diaminobutane^{2+} is interesting, since the length of the hydrocarbon chain and hence the distance between the two charges may be systematically varied. Such divalent molecules of varying length may provide a probe for exploring the location of ion binding sites within the aqueous pore (28).

DISCUSSION

Though extraordinarily selective in physiologic ion mixtures, Ca channels become freely permeable to all alkali metal ions when Ca^{2+} is removed. Here we report that after Ca^{2+}

removal, the Ca channel of skeletal muscle becomes permeable also to many organic cations, the largest being Me_4N^+ and the divalent 1,4-diaminobutane. The permeability of monovalent organic cations was found to be strongly determined by ion size, suggesting that, in the absence of Ca^{2+}, the Ca channel selects by a sieving mechanism. Hence, our results may be used to estimate the pore size. In order to pass Me_4N^+, the narrowest region in the aqueous pore must be at least as large as a 5.5 × 5.5 Å square or a 6-Å (diameter) circle. This leaves easily enough room for a Ca^{2+} and a H_2O molecule side by side (Fig. 4*b*). The pore is larger than in voltage-dependent Na channels, which exclude methylamine (20), or in delayed rectifier K channels, where NH_4^+ is the only organic cation known to be permeant (23). The pore size estimated here approaches that of the notoriously unselective, acetylcholine-activated channel at the neuromuscular junction (21). It is consistent with the idea that Ca channels achieve the high selectivity observed under physiologic conditions by selective binding of Ca^{2+} and not by rejection of monovalent cations.

Our measurements relied on Ca^{2+} removal for making Ca channels permeable to a variety of foreign cations. Hence, we cannot be sure that our estimate of pore size applies also at physiologic Ca^{2+} concentration. However, it seems fairly certain that this effect of Ca removal on permeability occurs by Ca^{2+} dissociating from sites that, located within the aqueous pore (4), are normal way stations for ions during permeation. Models based on this mechanism can account quantitatively for the observed permeability changes without assuming a change in pore size (6, 7). A similar mechanism has been established for the gramicidin A channel (11–14), which is normally permeable to all alkali metal ions but becomes selectively permeable to Tl^+ in ion mixtures. Though the pore in gramicidin A apparently widens when it complexes ions, the width of the pore appears to be independent of the type of ion present there (24). Hence, it is tempting to speculate that, in the presence of permeant ions, a pore diameter of at least 6.0 Å is a permanent feature of the open channel and applies to the Ca channel of skeletal muscle in the same way as other estimates of pore size apply to other channels. Whether other Ca channels have a similarly large pore remains to be seen; in neoplastic B lymphocytes, Me_4N^+ was reported to be impermeant (4). Similarly, the Mg^{2+} permeability observed in skeletal muscle (Fig. 1 and ref. 18) may be unusual for Ca channels (25).

It has been suggested that the paired Ca sites postulated to reside in the aqueous pore may be analogous to the paired Ca-specific sites on calmodulin and other Ca-binding proteins of this class (6, 7). In at least two of these proteins, parvalbumin and intestinal Ca-binding protein, the Ca-binding "pockets" snugly surround the ion in all directions but one (26, 27), a feature that is probably important for binding Ca^{2+} selectively and with high affinity. Our work shows that the pore of Ca channels can be considerably larger than the Ca-binding pockets of such proteins while they are occupied by Ca^{2+}.

We thank Drs. Bertil Hille and William M. Roberts for helpful discussions throughout this work and Dr. Hille for his suggestions on the manuscript. This research was supported by Grant AM-17803 from the National Institutes of Health.

1. Reuter, H. & Scholz, H. (1977) *J. Physiol. (London)* **264,** 17–47.
2. Lee, K. & Tsien, R. W. (1982) *Nature (London)* **297,** 498–501.
3. Almers, W., McCleskey, E. W. & Palade, P. T. (1984) *J. Physiol. (London)* **353,** 565–583.
4. Fukushima, Y. & Hagiwara, S. (1985) *J. Physiol. (London)* **358,** 255–284.
5. Kostyuk, P. G., Mironov, S. L. & Shuba, Ya. M. (1983) *J. Membr. Biol.* **76,** 83–93.
6. Almers, W. & McCleskey, E. W. (1984) *J. Physiol. (London)* **353,** 585–608.
7. Hess, P. & Tsien, R. W. (1984) *Nature (London)* **309,** 453–456.
8. Prosser, C. L., Kreulen, D. L., Weigel, R. J. & Yau, W. (1977) *Am. J. Physiol.* **233,** C19–C24.
9. Yoshida, S. (1983) *J. Physiol. (London)* **339,** 631–642.
10. Yamamoto, D. & Washio, H. (1979) *Can. J. Physiol. Pharmacol.* **57,** 220–223.
11. Neher, E. (1975) *Biochim. Biophys. Acta* **401,** 540–544.
12. Urban, B. W., Hladky, S. B. & Haydon, D. A. (1980) *Biochim. Biophys. Acta* **602,** 331–354.
13. Urry, D. W., Prasad, K. U. & Trapane, T. L. (1982) *Proc. Natl. Acad. Sci. USA* **79,** 390–394.
14. Urry, D. W., Venkatachalam, C. M., Spisni, A., Läuger, P. & Khaled, M. A. (1980) *Proc. Natl. Acad. Sci. USA* **77,** 2028–2032.
15. McCleskey, E. W. & Almers, W. (1984) *Biophys. J.* **47,** 66 (abstr.).
16. Hille, B. & Campbell, D. T. (1976) *J. Gen. Physiol.* **67,** 265–293.
17. Schwartz, L. M., McCleskey, E. W. & Almers, W. (1985) *Nature (London)* **314,** 747–751.
18. Almers, W. & Palade, P. T. (1981) *J. Physiol. (London)* **312,** 159–176.
19. Almers, W., Fink, R. & Palade, P. T. (1981) *J. Physiol. (London)* **312,** 177–207.
20. Hille, B. (1971) *J. Gen. Physiol.* **58,** 599–619.
21. Dwyer, T. M., Adams, D. J. & Hille, B. (1980) *J. Gen. Physiol.* **75,** 469–492.
22. Solomon, A. K. (1978) *J. Gen. Physiol.* **51,** 335–364.
23. Hille, B. (1973) *J. Gen. Physiol.* **61,** 669–686.
24. Koeppe, R. E., Berg, J. M., Hodgson, K. O. & Stryer, L. (1979) *Nature (London)* **279,** 723–725.
25. Hagiwara, S. & Byerly, L. (1981) *Annu. Rev. Neurosci.* **6,** 189–193.
26. Moews, P. C. & Kretsinger, R. H. (1975) *J. Mol. Biol.* **91,** 201–228.
27. Szebeny, D. M. E., Obendorf, S. K. & Moffat, K. (1981) *Nature (London)* **294,** 327–332.
28. Miller, C. (1982) *J. Gen. Physiol.* **79,** 869–891.